APPLIED PHYSICS LETTERS **89**, 033106 (2006)

# Special cantilever geometry for the access of higher oscillation modes in atomic force microscopy

S. Sadewasser
*Hahn-Meitner Institut, Glienicker Strasse 100, 14109 Berlin, Germany and Instituto de Microelectrónica de Barcelona, CNM-CSIC, Campus UAB, 08193 Bellaterra (Barcelona), Spain*

G. Villanueva and J. A. Plaza[a]
*Instituto de Microelectrónica de Barcelona, CNM-CSIC, Campus UAB, 08193 Bellaterra (Barcelona), Spain*

(Received 10 February 2006; accepted 26 May 2006; published online 18 July 2006)

Employing higher oscillation modes of microcantilevers promises higher sensitivity when applied as sensors, for example, for mass detection or in atomic force microscopy. Introducing a special cantilever geometry, we show that the relation between the resonance frequencies of the first and second resonance modes can be modified to separate them further or to bring them closer together. In atomic force microscopy the latter is of special interest as the photodiode of the beam deflection detection limits the accessible frequency range. Using finite element simulations, we optimized the design of the modified cantilever geometry for a maximum reduction of the frequency of the second oscillation mode with respect to the first mode. Cantilevers were fabricated by silicon micromachining and subsequently utilized in an ultrahigh vacuum Kelvin probe force microscope imaging the surface potential of $C_{60}$ on graphite. © *2006 American Institute of Physics*.
[DOI: 10.1063/1.2226993]

In the recent years, microcantilevers have been employed for sensor application in very versatile applications. The most widespread application is likely the cantilever as a supporting structure for the tip of an atomic force microscope (AFM), as first presented in 1986.[1] Other applications are in mass sensors,[2] as a sensor for gases and biomolecules,[3] or as the recently developed artificial nose[4] and millipede.[5] Many of the molecular detection devices are based on static cantilever bending due to the development of a surface stress as a result of the interaction between the molecules of interest. On the other hand, dynamic detection is more sensitive and therefore preferred in many applications, for example, in dynamic AFM (Ref. 6) or in mass sensors. Here the cantilever is vibrated close to its resonance frequency, and a change in the forces acting on the cantilever will modify its effective spring constant and its resonance frequency. This change can be used to calculate the mass change or can be used for a feedback to maintain a constant force when scanning a surface in dynamic AFM.

More recently, the possible advantages of using higher harmonics and higher eigenmodes of oscillation of cantilevers have received some attention. Stark[7] describes the appearance of higher harmonic oscillations due to increased tip-sample forces in tapping mode AFM. Sharos *et al.*[8] show that the sensitivity of mass detection can be increased by using higher oscillation modes, i.e., torsional modes of a regular AFM cantilever. Even earlier, the second mode of oscillation of an AFM cantilever was employed for the detection of the surface potential, simultaneously with the regular topography measurement in a Kelvin probe force microscope (KPFM).[9] In this method an ac bias at the frequency of the second oscillation mode is applied to the sample (or the tip), which induces cantilever oscillation at this frequency. If an additional dc bias is adjusted correctly to compensate for the electrostatic force between the tip and the sample, the oscillation at this frequency will vanish and the dc bias will correspond to the contact potential (CP) between the tip and the sample. This KPFM technique has been used to record CP images simultaneously with topography,[10–13] with the advantage that the higher sensitivity of a resonant detection allows us to use small amplitudes for the ac bias. A limiting factor regarding the cantilevers to be used in such applications is the bandwidth of the photodetector of the beam deflection detection system of the AFM equipment. In many experimental setups this is limited to ~500 kHz. An AFM cantilever usually consists of a rectangular beam of a few micrometer thickness, ~30 $\mu$m width, and 200–500 $\mu$m length; for this geometry the relation between the first ($f_1$) and the second ($f_2$) resonance mode of oscillation is $f_2/f_1 \sim 6.3$. Thus, the first resonance is limited to 80 kHz to ensure $f_2 < 500$ kHz.

In this letter we present a study of cantilevers with a modified geometry which results in a significant change of the ratio $f_2/f_1$. The resonance modes are simulated using finite element methods to optimize the geometry. Cantilevers were fabricated using silicon micromachining, and their proper operation was confirmed in an ultrahigh vacuum (UHV) KPFM.

The modified geometry consists of cantilevers divided into two parts, where the part anchored to the chip has a length $l_1$ and a width $w_1$ and the free part of the cantilever has length $l_2$ and width $w_2$. The whole cantilever has a homogeneous thickness $t$. The geometry is shown in the inset of Fig. 1(b). Cantilevers with this geometry were simulated using finite element methods (ANSYS), and the frequencies of the first and second oscillation modes were calculated for variations of the parameters $l_1$, $l_2$, $w_1$, $w_2$. The oscillation modes are shown in the inset of Fig. 1(b). For the fixed width ratio $w_2/w_1 = 20\ \mu\text{m}/60\ \mu\text{m}$, the frequency ratio $f_2/f_1$ as a function of the length ratio $l_2/(l_1+l_2)$ is shown in Fig. 1(a). The total length was maintained constant at $l_1+l_2=l_{\text{tot}} = 200\ \mu\text{m}$ and the thickness $t = 1\ \mu\text{m}$. The dependence of

---

[a] Electronic mail: joseantonio.plaza@cnm.es

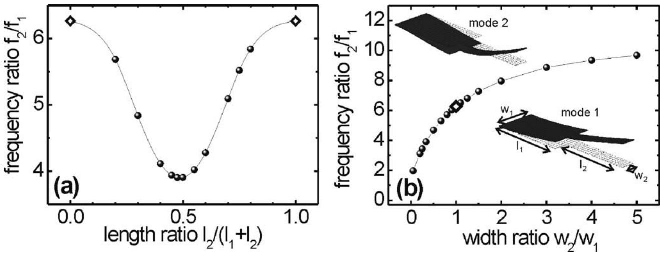

FIG. 1. Results of the ANSYS simulation of cantilevers with a modified geometry. (a) Ratio of the resonance frequencies of the first ($f_1$) and second ($f_2$) oscillation modes for a variation of the lengths of a wider anchored part $l_1$ ($w_1=60\ \mu$m) and a narrower free end $l_2$ ($w_2=20\ \mu$m) of the cantilever. A minimum in $f_2/f_1$ is observed for $l_1=l_2$. (b) Resonance frequency ratio $f_2/f_1$ for a variation of the width of the anchored part of a cantilever consisting of two equally long parts ($l_1=l_2=100\ \mu$m). The inset shows the oscillation modes.

$f_2/f_1$ clearly shows a minimum at $l_1=l_2$, when both parts have the same length of 100 $\mu$m. The ratio $f_2/f_1 \approx 6.3$ for the regular rectangular geometry is indicated by the open diamonds. In Fig. 1(b) we present the dependence of $f_2/f_1$ as a function of the width ratio $w_2/w_1$ maintaining the "optimal" length ratio $l_2/(l_1+l_2)=0.5$. The frequency ratio can be as low as 2 by increasing the width of the anchored part. On the other side, the ratio $f_2/f_1$ can be increased beyond 6.3 if the free end of the cantilever is designed wider than the anchored part. Both results are of interest. Lowering $f_2$ with respect to $f_1$ is desired for AFM applications, where the detection photodiode sets a limit for the highest frequency which can be detected; on the other hand, if detection is not a limitation, it is desirable to shift the resonances further apart to minimize cross talk. Simulation of the first torsional mode at the frequency $f_3$ shows an even stronger dependence of $f_3/f_1$ as a function of the length ratio $l_2/(l_1+l_2)$ and the width ratio $w_2/w_1$.[14]

Based on the described design optimization we have fabricated cantilevers for AFM application by silicon micromachining using inductively coupled plasma (ICP) dry etching processes and the parameters $l_1=l_2=100\ \mu$m, $w_1=60\ \mu$m, $w_2=20\ \mu$m, and $t=1\ \mu$m. A 15 $\mu$m silicon on insulator (SOI) wafer was provided with a circular $SiO_2$ mask for the formation of the tip using isotropic and anisotropic dry processes (Alcatel A601 model) reducing the thickness of the silicon layer to $\sim 1\ \mu$m. Using regular photoresist (HPIR-6512) and an additional dry process in the same equipment, the geometry of the cantilever is defined. Subsequently, the chip is defined using an aluminum mask on the backside of the wafer and a deep reactive ion etching (DRIE) is used to etch throughout the whole thickness of the wafer liberating the chip, which remains supported in the wafer by two small hinges. The oxide insulating layer of the SOI wafer serves as an etch stop for this step. Subsequently, this oxide is etched using HF vapors, which release the cantilever. Details of the fabrication process can be found in Ref. 14.

The chips with the cantilevers were mounted into a commercial AFM (Nanotec, Spain), and a frequency scan was performed to obtain the frequencies of the first and second oscillation modes. A typical frequency spectrum is presented in Fig. 2, showing the first resonance peak at $f_1=40.7$ kHz and the second mode at $f_2=136.6$ kHz. The peaks are fairly sharp; however, some noise in the frequency range between the resonances is observed. The frequency ratio results to $f_2/f_1=3.4$, slightly lower than the one expected from the simulation. Scanning electron microscopy images (inset of Fig. 2) revealed that the cantilevers suffered from considerable lateral etching due to the dry etching process, resulting in a final width $w_1=50\ \mu$m and $w_2=10\ \mu$m. Subsequent simulation of this geometry results in $f_2/f_1=3.2$, in close agreement with the experimentally obtained ratio. The quality factor of the fundamental oscillation mode can be determined from the width of the resonance peak to $Q=f/\Delta f \sim 45$, which is a reasonable value for cantilevers subject to damping in ambient air. The quality factor might also be influenced by the larger area of the cantilever end anchored to the chip. This could affect the minimum detectable force $F_n^{\min}=\sqrt{2k_B D_n T \Delta\omega / Q \pi \omega_n}$,[15] which depends on $Q$ ($k_B$-Boltzmann constant, $T$-temperature, $D_n$-spring constant of the $n$th eigenmode, and $\omega_n$-frequency of the $n$th eigenmode).

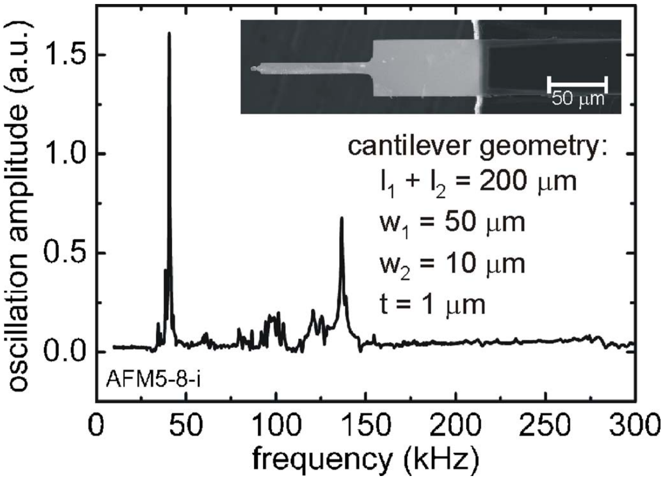

FIG. 2. (Color online) Frequency spectrum of a cantilever with modified geometry (parameters are given in the figure) using an AFM in ambient air, an excitation amplitude of 0.3 V, and a gain of 30. The fundamental resonance mode is at $f_1=40.7$ kHz and the second mode at $f_2=136.6$ kHz, resulting in a ratio $f_2/f_1=3.4$.

After the experimental confirmation of the changed frequency ratio for the modified cantilever geometry, we tested the cantilevers in a UHV-KPFM measuring a sample with topographic and surface potential contrast. The sample was a highly oriented pyrolytic graphite (HOPG) on which a submonolayer coverage of $C_{60}$ has been deposited using a vacuum evaporation system at room temperature.[16,17] The topography is measured using the frequency modulation technique at the resonance frequency of the first oscillation mode ($f_1=40.7$ kHz), and the CP using the second resonance mode ($f_2=136.6$ kHz) applying an ac bias of 50 mV. The topography in Fig. 3(a) shows several terraces with well defined steps between them; however, from this image it is not clear which parts of the sample are the HOPG substrate and where the deposited $C_{60}$ is located. The CP image in Fig. 3(b) shows a clear contrast between the two materials. The regions with the higher CP correspond to $C_{60}$ in agreement with previous findings.[16–18] The lateral resolution in topography and CP images is inferior to the resolution obtained with commercial tips. We attribute this to a not yet optimized tip formation process, which results in a slightly blunt tip. In the future the tip sharpness will be optimized. Nevertheless, Fig. 3 shows clearly that the cantilevers with the modified geometry and a reduced resonance frequency ratio $f_2/f_1$

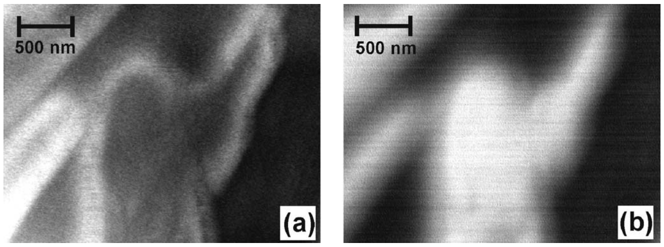

FIG. 3. UHV-KPFM image ($3.0\times 2.3\ \mu m^2$) of $C_{60}$ on HOPG. (a) The topography (gray scale=12 nm) shows several surface steps and (b) the CP image (gray scale=−140 to 10 mV) shows a clear contrast between $C_{60}$ (bright contrast) and HOPG (dark contrast).

=3.4 are well suited for their application in KPFM, allowing us to obtain high quality CP images.

Based on these results, cantilevers with $f_2$ close to the bandwidth of the photodetector can be fabricated, allowing a significant increase of the spring constant and resonance frequency of the first oscillation mode (up to $f_1 \sim 140$ kHz) and thus an increased stability of the topography measurement. The detection sensitivity in the beam deflection detection depends on the oscillation amplitude as well as on the deflection angle. As the mode shape of the modified geometry is similar to the mode shape of the rectangular cantilever, positioning the detection laser spot close to the end promises best detection sensitivity.[19]

We have proposed a novel geometry for cantilevers to be used in AFM when higher modes of oscillation are to be monitored to obtain information on additional sample properties. Changing the regular rectangular geometry to one consisting of a wider anchored part and a narrower free end, the frequency of the second mode of oscillation can be lowered with respect to the fundamental resonance mode, such that the frequency ratio $f_2/f_1$ is smaller than 6.3, as found for the rectangular geometry. The cantilevers were simulated to optimize the geometry and were subsequently fabricated using Si micromachining processes; the changes are easily included in the technological fabrication of cantilevers. This modified geometry can be used in AFM modulation experiments on higher eigenmodes, allowing sensitive detection of additional sample properties, as was demonstrated by the measurement of the contact potential of $C_{60}$ on the nanometer scale. Application in various sensor devices, for example, mass sensors, is also advantageous. First results on simulating variations of the cantilever thickness instead of the cantilever width suggest a similar effect on $f_2/f_1$; however, fabrication of such structures is more elaborate and complicated.

The authors gratefully acknowledge financial support from the Spanish government through the MINAHE project (TIC2002-04280-C03-02) and the MINAHE 2 project (TEC2005-07996-CO2-01).

[1] G. Binnig, C. F. Quate, and Ch. Gerber, Phys. Rev. Lett. **56**, 930 (1986).
[2] Z. J. Davis, G. Abadal, O. Kuhn, O. Hansen, F. Grey, and A. Boisen, J. Vac. Sci. Technol. B **18**, 612 (2000).
[3] H. Jensenius, J. Thaysen, A. A. Rasmussen, L. H. Veje, O. Hansen, and A. Boisen, Appl. Phys. Lett. **76**, 2615 (2000).
[4] M. K. Baller, H. P. Lang, J. Fritz, Ch. Gerber, J. K. Gimzewski, U. Drechsler, H. Rothuizen, M. Despont, P. Vettiger, F. M. Battiston, J. P. Ramseyer, P. Fornaro, E. Meyer, and H.-J. Güntherodt, Ultramicroscopy **82**, 1 (2000).
[5] U. Drechsler, N. Bürer, M. Despont, U. Dürig, B. Gotsmann, F. Robin, and P. Vettiger, Microelectron. Eng. **67/68**, 397 (2003).
[6] Y. Martin, C. C. Williams, and H. K. Wickramasinghe, J. Appl. Phys. **61**, 4723 (1987).
[7] R. W. Stark, Nanotechnology **15**, 347 (2004).
[8] L. B. Sharos, A. Raman, S. Crittenden, and R. Reifenberger, Appl. Phys. Lett. **84**, 4638 (2004).
[9] A. Kikukawa, S. Hosaka, and R. Imura, Appl. Phys. Lett. **66**, 3510 (1995).
[10] Ch. Sommerhalter, Th. W. Matthes, Th. Glatzel, A. Jäger-Waldau, and M. Ch. Lux-Steiner, Appl. Phys. Lett. **75**, 286 (1999).
[11] S. Sadewasser, Th. Glatzel, M. Rusu, A. Jäger-Waldau, and M. Ch. Lux-Steiner, Appl. Phys. Lett. **80**, 2979 (2002).
[12] Th. Glatzel, D. Fuertes Marrón, Th. Schedel-Niedrig, S. Sadewasser, and M. Ch. Lux-Steiner, Appl. Phys. Lett. **81**, 2017 (2002).
[13] O. Douhéret, S. Anand, Th. Glatzel, K. Maknys, and S. Sadewasser, Appl. Phys. Lett. **85**, 5245 (2004).
[14] S. Sadewasser, G. Villanueva, and J. A. Plaza, Rev. Sci. Instrum. (in press).
[15] S. Rast, C. Wattinger, U. Gysin, and E. Meyer, Rev. Sci. Instrum. **71**, 2772 (2000).
[16] S. Sadewasser, P. Carl, Th. Glatzel, and M. Ch. Lux-Steiner, Nanotechnology **15**, S14 (2004).
[17] S. Sadewasser and M. Ch. Lux-Steiner, Phys. Rev. Lett. **91**, 266101 (2003).
[18] The difference in CP between HOPG and $C_{60}$ is slightly higher than that found in Ref. 17, which is likely due to the storage of the sample in air for an extended time.
[19] T. E. Schäffer and H. Fuchs, J. Appl. Phys. **97**, 083524 (2005).